Synthesis of 6,6'-Bis{methyl[1-(2-hydroxyethyl)-piperazyl]}-2,2'-bipyridine and its Complexation with Co^{2+}, Ni^{2+}, Cu^{2+} and Zn^{2+} Ions

Vesa Hietapelto,* Riitta H. Laitinen, Risto S. Laitinen and Jouni Pursiainen

Department of Chemistry, University of Oulu, Linnanmaa, FIN-90570 Oulu, Finland

Hietapelto, V., Laitinen, R. H., Laitinen, R. S. and Pursiainen, J., 1999. Synthesis of 6,6'-Bis{methyl[1-(2-hydroxyethyl)piperazyl]}-2,2'-bipyridine and its Complexation with Co^{2+}, Ni^{2+}, Cu^{2+} and Zn^{2+} Ions. – Acta Chem. Scand. 53: 340–347. © Acta Chemica Scandinavica 1999.

6,6'-Bis{methyl[1-(2-hydroxyethyl)piperazyl]}-2,2'-bipyridine was synthesized, and its complex formation equilibria with cobalt(II), nickel(II), copper(II) and zinc(II) ions were studied with potentiometric techniques over the pH range 2.2–9.6 in 0.10 mol dm^{-3} NaCl at 25 °C. The data indicate the formation of the species [M(H$_X$L$_Y$)]$^{(2+X)+}$ ($X=0–3$ and $Y=1, 2$) and the hydrolysed [M(OH)$_X$L]$^{(2-X)+}$ complexes ($X=1, 2$). All the metal ions formed the [M(H$_2$L)]$^{4+}$ complexes, but Co^{II} and Zn^{II} also formed the [M(H$_3$L)]$^{5+}$ complexes. The protonation of the ligand and the complex formation were studied by ^{1}H NMR at 24 °C as well as by UV–VIS spectroscopy at 25 °C. These spectroscopic data, together with potentiometric results, can be used to discuss the conformational changes between the [M(H$_3$L)]$^{5+}$ and the [M(H$_2$L)]$^{4+}$ complexes.

2,2'-Bipyridine and its derivatives are well known for their ability to form stable coordination compounds with a large number of metal ions. Therefore 2,2'-bipyridine has become a widely used building block for large ligands that bind metal ions.[1] For example, macrocyclic polypyridine ligands allow the control of metal ion binding via ligand design.[2] 2,2'-Bipyridines and their metal complexes have a strong influence expecially on biological and non-biological catalytic processes.[1] For example, ruthenium–bipyridine compounds are widely studied because they are highly luminescent species and powerful reactants for light-induced and light-generating electron transfer processes.[3,4]

The structurally analogous ligands containing thiomorpholine and piperidine have previously been prepared.[5] These heterocycles are commonly used as building blocks in macrocyclic chemistry. These structures could allow a comparison of the complexes of related cyclic and open-chain structures. Because of the low water solubility of thiomorpholine- and piperidine-based complexes, we synthesized 6,6'-bis{methyl[1-(2-hydroxyethyl)piperazyl]}-2,2'-bipyridine (L$_1$), which is water-soluble and therefore suitable for traditional potentiometric titration in a constant ionic medium. Crystal structures, spectroscopic and NMR data of the complexes are known,[3-7] but thermodynamic

data are sparse. Crystal structures can be used to discuss the geometries of the complexes, but they do not give information about the thermodynamics or the selectivity of the complex formation. Piperazine is frequently used for the design of various ligands, since it contains two nitrogen atoms that can coordinate to metal ions.[6] It is less rigid than aromatic rings but more rigid than secondary amines when it acts as a double-bridged building block.[7] Piperazine and its N-substituted derivatives have pharmacological applications as anthelmintics, sedatives and local anaesthetics.[8] Transition metal ions chosen for the studies are of biological and catalytic interest. The metal cations also represent different affinities towards nitrogen donor ligands.[9]

Experimental

Synthesis. 6,6'-Bis(bromomethyl)-2,2'-bipyridine was synthesized as described previously.[5] 6,6'-Bis{methyl[1-(2-hydroxyethyl)piperazyl]}-2,2'-bipyridine (Fig. 1) was prepared by dissolving 6,6'-bis(bromomethyl)-2,2'-bipyridine (0.342 g, 1.0 mmol) in 20 cm^3 of a tetrahydro-furan–acetonitrile mixture (1:1 v:v) under mild heating, and by adding the resulting solution dropwise into 20 cm^3 of a tetrahydrofuran–acetonitrile (1:1 v:v) solution containing 1-(2-hydroxyethyl)piperazine (0.260 g, 2.0 mmol) and solid K$_2$CO$_3$ (0.553 g, 4.0 mmol). The reaction mixture was refluxed for 12 h. After cooling,

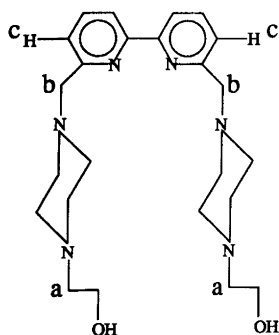---

* To whom correspondence should be addressed.

Fig. 1. The molecular structure of 6,6'-bis{methyl-[1-(2-hydroxyethyl)piperazyl]}-2,2'-bipyridine (L_1). **a** refers to the methylene protons of 2-hydroxyethyl chains, **b** refers to the methylene protons near the 2,2'-bipyridine unit, and **c** refers to the protons of 2,2'-bipyridine.

filtration and evaporation of the solvent, the brown residue was formed. It was dissolved in 10 cm^3 of a methanol–dichloromethane mixture (1 : 10 v : v) and separated by reversed-phase chromatography (LiChroprep RP-18, Merck) using methanol–dichloromethane (1 : 10 v : v) as eluent. The solvent was subsequently evaporated. The product was obtained as a brown–yellow oil. Yield 0.298 g (68%). The elemental analysis imply that the product contains ca. 97% of $C_{24}H_{36}N_6O_2$ and ca. 3% residue of KBr that was formed in the reaction. Anal. Calcd. for $C_{24}H_{36}N_6O_2$: C, 65.4; H, 8.2; N, 19.1%. Found: C, 63.4; H, 7.8; N, 18.1%. The AgNO$_3$ test indicates that ca. 3% of the product can be KBr. Anal. Calcd for this mixture: C, 65.4; H, 8.0; N, 18.7%. m/z 440 (M^+), 312 $(M-C_6H_{12}N_2O)$, 281 $(M-[C_6H_{12}N_2O+CH_3O])$, 227 $(M-[C_6H_{12}N_2O+C_4H_7NO])$, 212 $(M-[C_6H_{12}N_2O+C_5H_{10}NO])$, 184 $(M-2\times C_6H_{12}N_2O)$. δ_H (200 MHz; solvent CDCl$_3$; standard SiMe$_4$) 2.56 [4 H, t, J(HH) 5.7 Hz, $-CH_2-CH_2-OH$], 2.61 (16 H, s, piperazine), 3.63 [4 H, t, J(HH) 5.4 Hz, $-CH_2-CH_2-OH$], 3.78 (4 H, s, Bipy-CH_2-piperazine), 7.44 [2 H, d, J(HH) 7.3 Hz, Bipy-H], 7.78 [2 H, t, J(HH) 7.8 Hz, Bipy-H], 8.27 [2 H, d, J(HH) 7.7 Hz, Bipy-H].

Reagents and solutions. Stock solutions of cobalt(II), nickel(II), copper(II) and zinc(II) ions were prepared from chlorides (Merck). These stock solutions were standardized by titration with EDTA as well as by cation exchange chromatography.[10] The purity of the ligand was determined by ^{1}H NMR spectroscopy and by titration of an acidified ligand with standardized NaOH solution. Hydrochloric acid (Baker) was standardized by titration with tris(hydroxymethyl)aminomethane (TRIS) using bromocresol green–methyl red (3 : 2) as an indicator. The NaOH stock solution was prepared by dissolving NaOH granules (Merck) in boiling distilled water. It was stored in a high-density polyethene bottle fitted with a carbon dioxide (soda lime) trap. The NaOH stock solution was standardized by titration of potassium hydrogen phthalate with it using phenolphtalein as an indicator.

Potentiometric studies. The potentiometric studies were carried out in an inert atmosphere [commercial argon passed through 10% (w/w) H$_2$SO$_4$, 10% (w/w) NaOH and background electrolyte] at 25 ± 0.1 °C using a locally constructed automatic titration system (TIT5 program)[11] involving a Methrohm 665 piston burette as well as an Orion 91-01sc glass electrode and an Orion 9002 Ag/AgCl(s) double-junction reference electrode. The ligand and metal ion concentrations as well as the pH range are given in Table 1. Every titration was started with the calibration of the electrode system by titration of 30 or 40 cm^3 of E_0-solution (0.090 and 0.010 M with respect to NaCl and HCl, respectively) with CO$_2$-free 0.10 M NaOH solution. These data were employed to obtain the value of E_0 (mV) in the Nernst equation

$$E = E_0 + 59.16 \log h + E_j \tag{1}$$

where h is the concentration of free H$^+$. The liquid junction potentials $[E_j = j_{ac}h + (j_{alk}k_w)/h]$ were determined by separate titrations and the obtained values $[j(\text{acid}) = -512 \pm 8$ mV M^{-1}, $j(\text{alk}) = 239 \pm 10$ mV M^{-1} and p$k_w = 13.775$] were similar to the literature values.[12]

Table 1. Experimental parameters: n_T = number of titrations, n_P = number of titration points, C_L = ligand concentration, C_M = metal ion concentration, M/L = metal to ligand concentration ratio.

Compound, method	n_T/n_P	M/L	C_L/mmol dm^{-3}	C_M/mmol dm^{-3}	pH range
L, protonation, pot	2/104	—	1.972–2.334	—	2.3–9.2
L, protonation, ^{1}H NMR	1/14	—	3.558	—	1.9–9.0
Zn^{II}, ^{1}H NMR	1/13	1 : 1	4.043	3.987	2.2–8.0
Co^{II}, VIS	1/12	1 : 1	5.391	5.373	2.1–8.0
Co^{II}, UV	1/8	1 : 1	0.05391	0.05373	2.0–7.4
Ni^{II}, VIS	1/14	1 : 1	10.390	10.313	2.1–8.5
Ni^{II}, UV	1/9	1 : 1	0.05195	0.05157	2.1–8.6
Cu^{II}, VIS	1/10	1 : 1	10.234	10.233	2.5–7.0
Cu^{II}, UV	1/7	1 : 1	0.05117	0.05117	2.5–6.8
Zn^{II}, UV	1/9	1 : 1	0.05391	0.05316	2.1–8.6
Zn^{II}, UV	1/11	1 : 2	0.05540	0.02731	2.2–8.9
Co^{II}, pot	3/156	1 : 1, 2 : 1, 1 : 2	1.285–2.771	1.325–2.614	2.4–8.9
Ni^{II}, pot	3/148	1 : 1, 2 : 1, 1 : 2	1.332–2.817	1.376–2.741	2.4–8.4
Cu^{II}, pot	3/155	1 : 1, 2 : 1, 1 : 2	1.285–2.771	1.329–2.622	2.2–9.6
Zn^{II}, pot	3/164	1 : 1, 2 : 1, 1 : 2	1.285–2.771	1.311–2.586	2.4–8.8

E_j, however, assumed a significant value only at pH <2.5. The titrations were mainly carried out under conditions where the liquid junction potential is negligible. The acidified solutions of the ligand (H_4L^{4+}) were titrated with NaOH to obtain the protonation constants and the exact ligand concentrations. The acidified solutions containing the ligand and the metal ion were titrated with NaOH to high pH to determine the stability constants of the metal complexes. The reversibility was tested by titrating with HCl back to low pH.

^{1}H NMR studies. The protonation measurements were carried out on a Bruker AM 200 spectrometer operating at 200.13 MHz for ^{1}H at $24 \pm 1\,°C$. In order to reach a sufficiently good signal-to-noise ratio, 128 FIDs were accumulated by applying a pulse width of 2.5 µs (nuclear tip angle of ca. 30°), a pulse delay of 5.7 s and spectral width of 3.5 kHz resulting in the resolution of 0.365 Hz/point. The protonation and Zn^{II} complexation chemical shifts were determined using the batch technique. The pH of each sample solution was adjusted with concentrated HCl and NaOH solutions and monitored with a combination electrode and Metler Toledo 320 pH meter [pH 4.01 and 6.87 buffers (TAMRO)] at room temperature ($24\,°C$). The spectra were recorded in a 5-mm tube directly from the water solution within a day after the pH adjustment to mimic the potentiometric titration. C_6D_6 was used as an external ^{2}H lock and TMS as an external reference. Solvent peak suppression was carried out by the presaturation method.

UV/VIS studies. UV/VIS spectra were recorded with a Philips PU 8740 scanning spectrophotometer using matched quarts cells of 10 mm path length at $25 \pm 0.1\,°C$. Visible spectra were scanned in the wavelength range 350–900 nm and the UV spectra in the range 190–400 nm. The pH of each sample solution was adjusted with concentrated HCl and NaOH solutions.

Calculations

Potentiometric titrations, ^{1}H NMR and UV/VIS spectroscopic measurements were carried out with the ligand concentration range indicated in Table 1. The protonation constants of the ligand and the stability con-

stants of complexes were calculated from the potentiometric data with program LETAGROPVRID, version ETITR,[13–15] and from the ^{1}H NMR data with the program SIGMAPLOT.[16] The modelling of the protonation equilibria on the basis of ^{1}H NMR data was carried out as described previously.[17] The hydrolysis of cobalt, copper and zinc ions were taken into account by assuming the constants $\log \beta_{Co(OH)^+} = -9.90 \pm 0.05$, $\log \beta_{Co(OH)_2} = -19.05 \pm 0.1$, $\log \beta_{Cu_2(OH)_2^{2+}} = -10.61 \pm 0.05$, $\log \beta_{Zn(OH)^+} = -9.21 \pm 0.05$ and $\log \beta_{Zn(OH)_2} = -17.2$.[18] The best fit to the experimental data was determined by minimizing the error square sum $U = \Sigma(H_{calc} - H_{exp})^2$, where H is the total hydrogen ion concentration or the ^{1}H chemical shift in the case of potentiometric titrations and NMR measurements, respectively. Every metal ion–ligand system has been modelled by the computer program SOLGASWATER.[19] Theoretical $Z(A/B)$ (the average number of protons bound to each ligand) versus $-\log[H^+]$ curves were calculated using this program to evaluate the correctness of the model.[20]

Results and discussion

Protonation. The logarithms of the protonation constants are presented in Table 2. The potentiometric and ^{1}H NMR data lead to similar protonation constants, though the pH measurements were performed in the concentration and activity scales in the case of potentiometric titrations and NMR experiments, respectively. The first and the second protonation take place in piperazine nitrogen atoms near the 2-hydroxyethyl chains, and the third and the fourth protonation in piperazine nitrogen atoms near bipyridine unit. The protonation of the bipyridine nitrogen donor atoms could not be confirmed. The protonation constants $\log \beta_{11}$ and $\log \beta_{12}$ were calculated using the methylene proton resonance of the 2-hydroxyethyl chains (resonance **a** in Fig. 2), and $\log \beta_{13}$ and $\log \beta_{14}$ were calculated using the methylene proton resonance of the bridge between bipyridine unit and piperazine rings (resonance **b** in Fig. 2).

Complexation. Logarithms of overall stability constants are shown in Table 3. $Z(A/B)$ versus $-\log[H^+]$ for Co^{II}-L_1 is presented in Fig. 3. The potentiometric data indicate that when $Z(A/B) \geqslant 2$, $[M(H_3L)]^{5+}$ and $[M(H_2L)]^{4+}$

Table 2. The protonation constants β_{qr} ($\pm \sigma$)^a and $K_{qr}{}^a$ of 6,6′-bis{methyl[1-(2-hydroxyethyl)piperazyl]}-2,2′-bipyridine at $25\,°C$ and $l = 0.10\ \text{mol dm}^{-3}$ NaCl, as determined using potentiometric titration and ^{1}H NMR spectroscopy.^{b}

	$\log \beta_{11}$	$\log \beta_{12}$	$\log \beta_{13}$	$\log \beta_{14}$	U^c
Potentiometric	7.91 (0.01)	14.88 (0.01)	18.73 (0.01)	21.28 (0.01)	6.7×10^{-3}
^{1}H NMR	7.86 (0.02)	15.00 (0.02)	18.86 (0.01)	21.63 (0.01)	3.13
	$\log K_{11}$	$\log K_{12}$	$\log K_{13}$	$\log K_{14}$	U
Potentiometric	7.91 (0.01)	6.97 (0.01)	3.85 (0.01)	2.55 (0.01)	6.7×10^{-3}
^{1}H NMR	7.86 (0.02)	7.14 (0.02)	3.86 (0.01)	2.77 (0.01)	3.13

$^a \beta_{qr}$ refers to the reaction $qL + rH = L_qH_r$ and K_{qr} refers to the reactions $L + H = LH$, $LH + H = LH_2$, $LH_2 + H = LH_3$ and $LH_3 + H = LH_4$. ^{b} ^{1}H NMR spectroscopic measurements have been carried out at $24\,°C$. ^{c}The error square (see calculations).
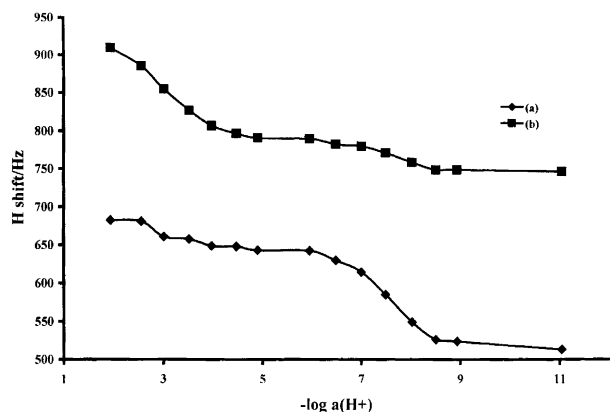
Fig. 2. Experimental chemical shift (Hz) vs. $-\log a_{H^+}$ of 6,6'-bis{methyl[1-(2-hydroxyethyl)piperazyl]}-2,2'-bipyridine at 24 °C and $I = 0.10\ mol\ dm^{-3}$ NaCl. **a** and **b** are defined in Fig. 1.
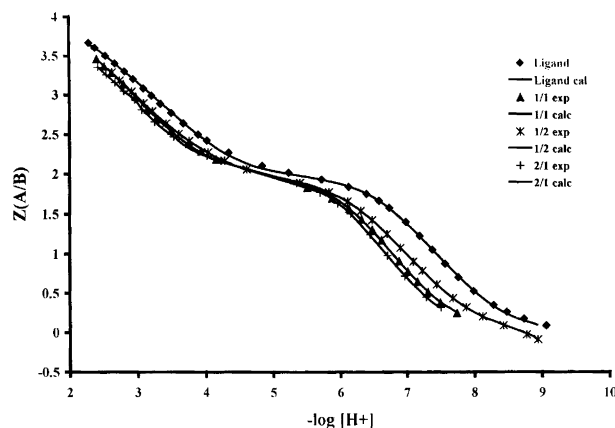
Fig. 3. $Z(A/B)$ (the average number of protons bound to each ligand) vs. $-\log[H^+]$ for Co^{II}-6,6'-bis{methyl[1-(2-hydroxyethyl)piperazyl]}-2,2'-bipyridine.

Table 3. The overall stability constants, β_{pqr} ($\pm \sigma$),[a] of Co^{II}, Ni^{II}, Cu^{II} and Zn^{II} with 6,6'-bis{methyl[1-(2-hydroxyethyl)piperazyl]}-2,2'-bipyridine at 25 °C and $I = 0.10\ mol\ dm^{-3}$ NaCl.

Metal ion	Species/$p\ q\ r$	$\log \beta_{pqr}$	U	$\log K_a{}^b$
Co^{II}	1 1 0	5.03 (0.01)	7.1×10^{-3}	—
	1 1 1	12.08 (0.01)	7.1×10^{-3}	7.05
	1 1 2	18.22 (0.01)	7.1×10^{-3}	6.14
	1 1 3	21.34 (0.02)	7.1×10^{-3}	3.12
	1 2 0	7.55 (0.03)^c	1.2×10^{-2}	—
	1 1 −2	−13.53 (0.02)^c	1.2×10^{-2}	−18.56
Ni^{II}	1 1 0	5.45 (0.02)	5.1×10^{-2}	—
	1 1 1	12.39 (0.02)	5.1×10^{-2}	6.94
	1 1 2	18.41 (0.02)	5.1×10^{-2}	6.02
Cu^{II}	1 1 0	9.36 (0.01)	2.5×10^{-2}	—
	1 1 1	15.57 (0.02)	2.5×10^{-2}	6.21
	1 1 2	20.92 (0.01)	2.5×10^{-2}	5.35
	1 2 0	11.07 (0.05)^c	5.2×10^{-2}	—
	1 1 −1	−0.07 (0.02)^c	5.2×10^{-2}	−9.43
Zn^{II}	1 1 0	6.11 (0.01)	1.2×10^{-2}	—
	1 1 1	13.00 (0.01)	1.2×10^{-2}	6.89
	1 1 2	19.08 (0.01)	1.2×10^{-2}	6.08
	1 1 3	21.83 (0.01)	1.2×10^{-2}	2.75
	1 2 0	8.15 (0.04)^c	1.7×10^{-2}	—
	1 1 −1	−2.31 (0.02)	7.3×10^{-3}	−8.42
	1 1 −2	−12.47 (0.06)^c	1.7×10^{-2}	−18.58

[a] β_{pqr} refers to the reaction $pM + qL + rH = M_pL_qH_r$. [b] K_a is the protonation constant of the complex (for example, $ML + H \rightleftharpoons MHL$: $\log \beta_{MHL} - \log \beta_{ML} = \log K_a(MHL)$. [c] $M/L = 1/2$.

complexes are present in the solution before the equivalent point, when $2 > Z(A/B) \geqslant 1$, the $[M(HL)]^{3+}$ complex is present in solution, and when $Z(A/B) < 1$, the $[ML]^{2+}$, $[ML_2]^{2+}$ and possible hydrolysed complexes exist in solution. The calculations were performed both on the whole data set and separately on the data with $Z(A/B) \geqslant 2$ and $Z(A/B) < 2$. The results are similar in the both cases. The best fit between the experimental and calculated $Z(A/B)$ values (dependent on $-\log[H^+]$) is obtained, when the $[ML_2]^{2+}$ and the hydrolysed complexes are included in the thermodynamic model.

All metal ions form $[M(H_2L_1)]^{4+}$ complexes with the H_4L^{4+} form of the ligand displacing two protons from the piperazine nitrogen atoms $[M^{2+} + H_4L^{4+} \rightleftharpoons$

$[M(H_2L)]^{4+} + 2H^+]$. It can be inferred from Fig. 1 that bipyridine nitrogen donor atoms and piperazine nitrogen donor atoms may form an approximately square planar coordination sphere as shown in Fig. 4(a).* Cobalt and zinc ions, which have different affinities to nitrogen donor atoms from nickel and copper ions, also form a $[M(H_3L)]^{5+}$ complex. In these complexes three piperazine nitrogen atoms are protonated and the coordination sphere around the metal ion contains only three nitrogen

---

* The geometry of the coordination, however, is not so clearly defined in solutions as in the crystalline state,[9] because the solvent molecules, hydroxide ions and chloride ions, as well as the polydentate ligand, can render the coordination to octahedral.
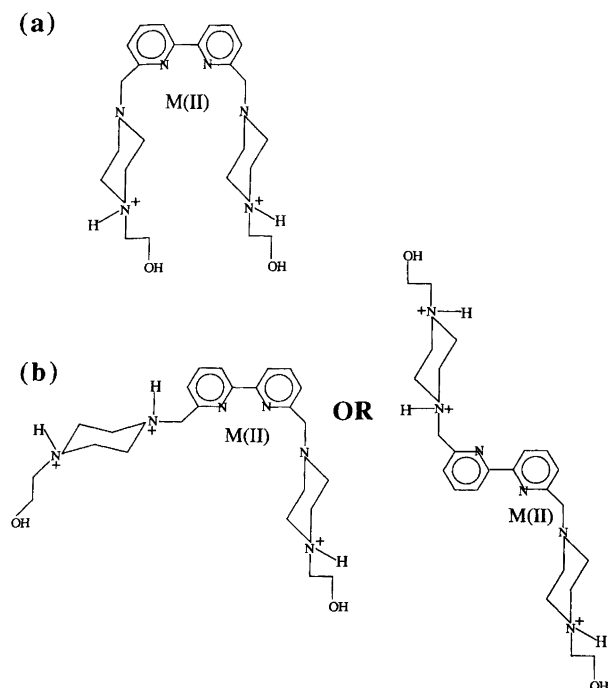
(a)

(b)

OR

Fig. 4. The possible coordination modes of the transition metal complexes of 6,6'-bis{methyl[1-(2-hydroxyethyl)-piperazyl]}-2,2'-bipyridine: (a) $[M(H_2L)]^{4+}$ and (b) $[M(H_3L)]^{5+}$.

Fig. 5. The distribution diagrams for the individual $[Co^{II}$-$L_1]$ titrations: (a) M : L = 1 : 1 and (b) M : L = 1 : 2.

atoms. If the bonding takes place through one bipyridine nitrogen donor as shown in Fig. 4(b), the coordination sphere around the metal ion contains only two nitrogen atoms. It is also possible that only bipyridine nitrogen atoms coordinate to cobalt and zinc ions. While nickel forms the $[M(H_2L)]^{4+}$ complex, it does not form a $[ML_2]^{2+}$ complex unlike other cations studied in this work. In neutral and basic conditions, where the $[ML_2]^{2+}$ complex could be formed, Ni^{II} species were precipitated due to hydrolysis. The equilibria were reached only slowly especially when $Z(A/B) > 2$. The kinetic phenomenona in the chelate formation of Ni^{II} are well known in water as well as in non-aqueous and mixed aqueous solvents.[21,22] The rate-determining step of the complexation is the formation of the monodentate intermediate through one bipyridine nitrogen atom, and it is followed by a rapid ring closure to give the chelate structure in water. On the other hand, the two different coordination models can compete simultaneously, when $Z(A/B) > 2$. The $[Co(H_3L_1)]^{5+}$ and $[Co(H_2L_1)]^{4+}$ complexes exist simultaneously, when pH < 4 (Fig. 5). The behaviour of Zn^{II} is analogous to Co^{II} according to potentiometric results. This was verified by use of ^1H NMR. The chemical shifts (in Hz) of the protons (c) and (b) for ligand and the Zn^{II} complexes vs. $-\log a_{H^+}$ are presented in Fig. 6. Two resonances (c1 and c2 or b1 and b2) can be seen in the Zn^{II}-L_1 when pH < 3.5 and only one resonance (c1 or b1) when pH > 3.5. This clearly shows that the two different species that have different coordination spheres exist when pH ⩽ 3.5.
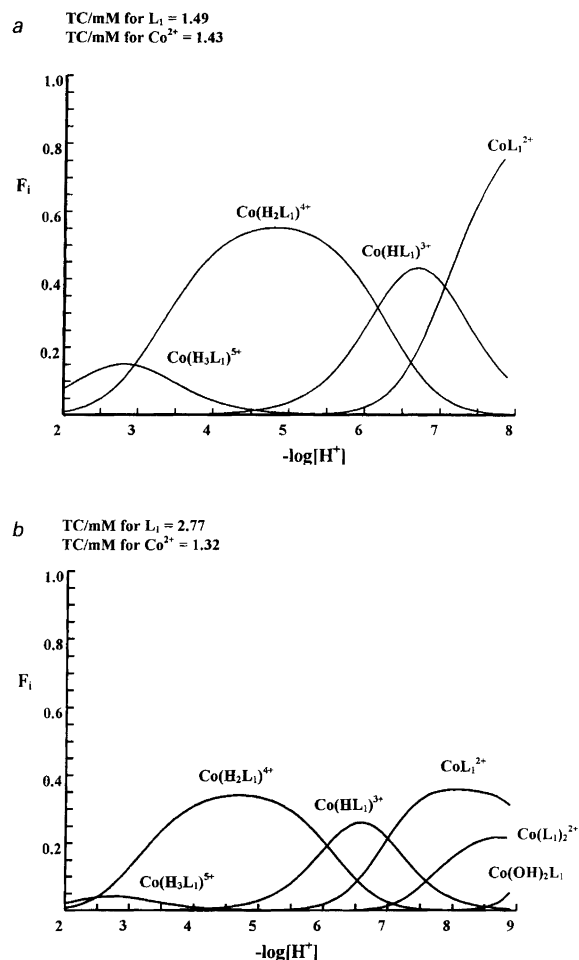
The order of the stability of the 6,6'-bis{methyl[1-(2-

hydroxyethyl)piperazyl]}-2,2'-bipyridine complexes is $Co^{II} < Ni^{II} < Zn^{II} < Cu^{II}$ that is in agreement with Irving–Williams order.[23,24] Similar order can also be seen among the protonated and hydroxo complexes. The log β of $[CuL]^{2+}$ is about three orders of the magnitude higher than that for the next stable $[ZnL]^{2+}$ complex, whereas the differences between the stability constants of corresponding cobalt, nickel and zinc complexes are smaller. The larger stability difference between the Cu^{II} and the other transition metal ions possibly results from the Jahn–Teller effect[25] when L_1 forms a square planar complex with Cu^{II} and the weakly coordinating water molecules occupy the axial positions forming a distorted octahedron. It has been reported that the log K value for the 6,6'-dimethyl-2,2'-bipyridine copper(II) complex $[CuL]^{2+}$ is 4.88 in 50% (W) water–dioxan mixture.[26] Those for the corresponding 4,4'-dimethyl-2,2'-bipyridine cobalt and zinc complexes are 6.38[27] and 6.0,[28] respectively. The stability of the 4,4'-dimethyl-2,2'-bipyridine cobalt complex is higher than that of the L_1 complex and the stability of the corresponding zinc complex is similar to the L_1 complex. The stability constants for the 4,4'-dimethyl-2,2'-bipyridine Co^{II} and Zn^{II} $[ML_2]^{2+}$ com-
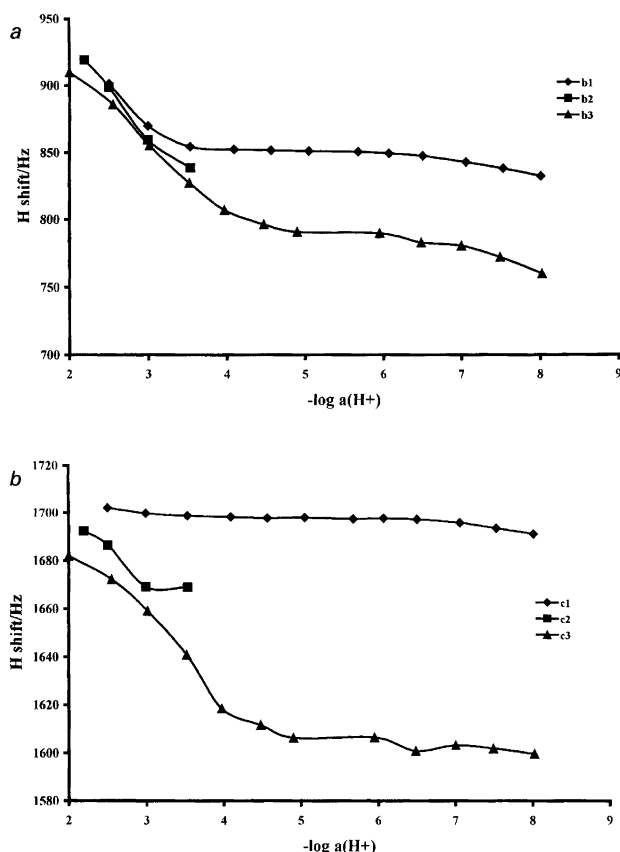
Fig. 6. The ^{1}H chemical shift (Hz) vs. $-\log a_{H^+}$ at 24 °C and $I = 0.10$ mol dm^{-3} NaCl: Zn^{II}-L$_1$ (c1, c2 and b1, b2) and L$_1$ (c3 and b3). c and b are defined in Fig. 1. The numerical indices 1 and 2 refer to the two observed proton resonances of Zn^{II}-L$_1$ complexes and 3 refers to the proton resonance of the L$_1$.

plexes are higher than those for the complexes of L$_1$, which is not unexpected, since the large piperazine fragments in the L$_1$ have a steric hindrance for the formation of the [ML$_2$]$^{2+}$ complexes compared to 4,4′-dimethyl-2,2′-bipyridine. The bipyridine unit seems to dominate the complexation of the L$_1$ with transition metal ions. This corresponds well with the known high affinity of 2,2′-bipyridine towards a large number of metal ions. The reduction of Cu^{II} to Cu^I is easy for the 6,6′-dimethyl-2,2′-bipyridine [CuL]$^{2+}$ in 50% (W) water–dioxan mixture.[26] This kind of reduction, however, should create strong charge-transfer bands in the UV spectrum.[9] In our case we did not observe those bands and infer that the reduction from Cu^{II} to Cu^I is not likely to happen in the Cu^{II}-L$_1$ complexes.

The distribution diagrams of M^{II} are exemplified by that of Co^{II} (Fig. 5). It can be seen that [Co(H$_3$L)]$^{5+}$ complex is quite rare when pH ⩽ 3 and the [Co(H$_2$L)]$^{4+}$ complex becomes more abundant when pH > 4. The Zn^{II} complexes behave in the same manner. In contrast, [Cu(H$_2$L)]$^{4+}$ is relatively abundant, when pH ⩽ 3. The [ML]$^{2+}$ and [ML$_2$]$^{2+}$ complexes as well as hydrolysed complexes clearly exist simultaneously when M : L = 1 : 2.

The [M(OH)$_2$L] complexes of Co^{II} and Zn^{II} are minor species (< 10%), but relative amount of the [Cu(OH)L]$^+$ complex is higher and it is the major species when pH > 8.5. The log K_2 values (ML + L ⇌ ML$_2$; log β_{ML_2} − log β_{ML} = log K_2; Table 3) are: Co^{II} 2.52, Cu^{II} 1.71, and Zn^{II} 2.04. These constants show that the higher the stability constant of the [ML]$^{2+}$ complex the lower the stability constant of the [ML$_2$]$^{2+}$ complex.

The protonation constants (log K_a) of the metal complexes (Table 3) are lower than the corresponding stepwise protonation constants of L$_1$ (Table 2). It can also be seen that the higher the stability constant of the [ML]$^{2+}$ complex the more acidic are the protonated metal complexes. The protonation constants of the hydrolysed metal complexes show a similar trend except for the [Zn(OH)$_2$L] complex.

UV–VIS spectroscopy. The UV spectra of the copper and zinc comples at different pH values are shown in Figs. 7(a) and (b). The UV spectroscopic results together with ^{1}H NMR results clearly verify the proposed changes in the coordination sphere between the [M(H$_3$L)]$^{5+}$ and [M(H$_2$L)]$^{4+}$ complexes, as shown in Fig. 4. Nickel has the analogous spectra with copper, and those of cobalt with zinc. It means that they have quite similar complex formation models. The M : L = 1 : 2 spectra of zinc are similar to those of the M : L = 1 : 1 spectra. The L$_1$ shows three absorption bands at ca. 202, 238 and 288 nm that do not appreciably depend on the pH. The absorption bands at 238 and 288 nm are assigned to 2,2′-bipyridine unit.[29] These two absorption bands do not shift during the protonation, therefore, the 2,2′-bipyridine unit in L$_1$ does not protonate. The Cu^{II}-L$_1$ absorption bands also vary only very slightly (the 2,2′-bipyridine bands at 246.4–250.2 nm and at 306.9–308.0 nm) [Fig. 7(a)] and we do not detect the isosbestic point. That possibly means that there are no significant exchange processes in the coordination sphere at this pH range. The absorption bands of the 2,2′-bipyridine unit in Zn^{II}-L$_1$ vary more clearly than in the case of Cu^{II}-L$_1$, varying 238.3 − 244.3 and 287.8–303.7 nm. A hydrolysed [Zn(OH)L]$^{1+}$ complex is formed, when pH > 7. We then observe an additional band at ca. 316 nm [Fig. 7(b)]. The isosbestic points are observed at 245.5 and 295.0 nm. Evidently the Zn^{II} complexes show a more complicated solution behaviour than the Cu^{II} complexes.

We were only able to record the visible spectra for the copper complexes, because the tail of the very intense, broad band of L$_1$ at ca. 300 nm spreads to the visible region and obscures the weak absorption bands of cobalt and nickel complexes. The visible spectra of the copper complexes are shown in Fig. 8. The Cu^{II} itself has the absorption band at 800–810 nm depending on the pH of the solution. It forms very intense green coloured complexes with L$_1$ and the wavelength of the absorption maximum varies from 742.2 to 695.2 nm as the pH is increased from 2.5 to 7.0. There is an isosbestic point at
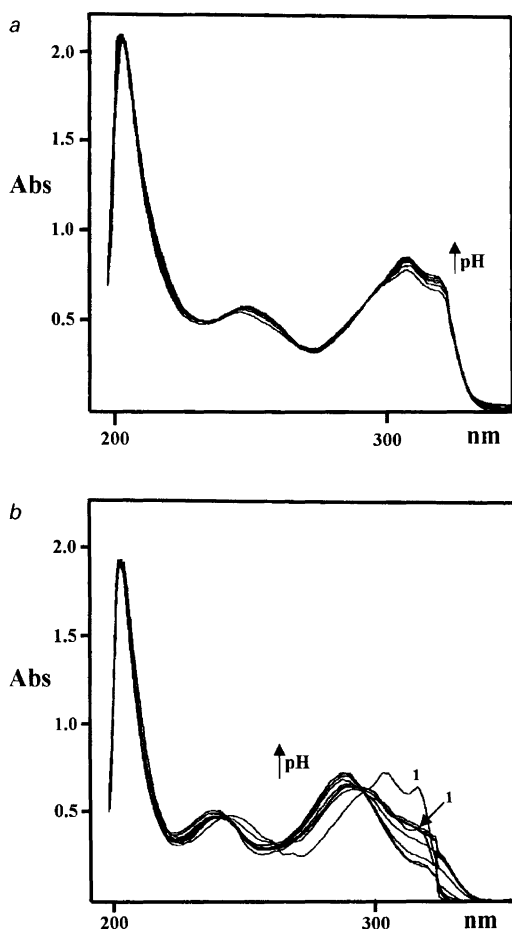
Fig. 7. The UV absorption spectra of [Cu^{II}-L$_1$] and [Zn^{II}-L$_1$] M:L = 1:1 vs. −log a_{H^+} at 25 °C and I = 0.10 mol dm^{-3} NaCl. (a) [Cu^{II}-L$_1$]. In the whole wavelength range pH increases from 2.54 to 6.72 in the direction of the arrow. (b) [Zn^{II}-L$_1$]. In the wavelength region 260–290 nm the pH increases from 2.26 to 6.18 in the direction of the arrow. (1) refers to the absorption maximum at 316 nm when pH is 7.20 or 8.63. The isosbestic points lie at 245.5 and 295.0 nm.
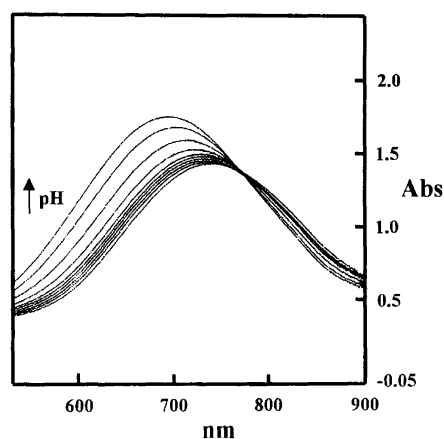

Fig. 8. The visible absorption spectra of [Cu^{II}-L$_1$] M:L = 1:1 vs. −log a_{H^+} at 25 °C and I = 0.10 mol dm^{-3} NaCl. In the wavelengths before 775 nm pH increases from 2.57 to 7.01 in the direction of the arrow. The isosbestic point lies at 775.0 nm.

775.0 nm that indicates that this system comprises two or more metal complexes.[30–32]

References

1. Vögtle, F. *Supramolecular Chemistry: an Introduction,* 1st Edn., John Wiley and Sons, Chichester 1991, pp. 9–26.
2. Rodriques-Ubis, J. C., Alpha, B., Plancherel, D. and Lehn, J. M. *Helv. Chim. Acta 67* (1984) 2264.
3. De Cola, L., Belser, P., Ebmeyer, F., Barigelletti, F., Vögtle, F., Zelewsky, A. and Balzani, V. *Inorg. Chem. 29* (1990) 495.
4. Opperman, K. A., Mecklenburg, S. L. and Meyer, T. J. *Inorg. Chem. 33* (1994) 5295.
5. Laitinen, R. H., Csoban, K., Pursiainen, J., Huuskonen, J. and Rissanen, K. *Acta Chem. Scand. 51* (1997) 462.
6. (a) Rissanen, K., Breitenbach, J. and Huuskonen, J. *J. J. Chem. Soc., Chem. Commun.* (1994) 1265; (b) Allinger, N. L., Carpenter, J. G. D. and Karkowski, F. M. *J. Am. Chem. Soc. 87* (1965) 1232; (c) Schneider, H. J. *Angew. Chem., Int. Ed. Engl. 30* (1991) 1417; (d) Wade, P. W. and Hancock, R. D. *J. Chem. Soc., Dalton Trans.* (1990) 1323; (e) Hancock, R. D., Ngwenya, M. P., Evers, A., Wade, P. W., Boyens, J. C. A. and Dobson, S. M. *Inorg. Chem. 29* (1990) 264; (f) Hancock, R. D., Dobson, S. M., Evers, A., Wade, P. W., Ngwenya, M. P., Boyens, J. C. A. and Wainwright, K. P. *J. Am. Chem. Soc. 110* (1988) 2788; (g) Wade, P. W., Hancock, R. D., Boyens, J. C. A. and Dobson, S. M. *J. Chem. Soc., Dalton Trans.* (1990) 483.
7. (a) Huuskonen, J., Schulz, J. and Rissanen, K. *Liebigs Ann.* (1995) 1515; (b) Larkins, H. L. and Hamilton, A. D. *Tetrahedron Lett. 27* (1986) 2721; (c) Krakowiak, K. E., Bradshaw, J. S., Jiang, W., Dalley, N. K., Wu, G. and Izatt, R. M. *J. Org. Chem. 56* (1991) 2675; (d) Saigo, K. *Chem. Lett.* (1989) 1289; (e) Ramasubbu, A. and Wainwright, K. P. *J. Chem. Soc., Chem. Commun.* (1982) 277; (f) Chenevert, R. and Plate, R. *Synthesis* (1983) 847; (g) Bazzicalupi, C., Benzini, A., Fusi, V., Micheloni, M. and Valtancoli, B. *J. Chem. Soc., Chem. Commun.* (1994) 1119.
8. Kushner, S. *J. Org. Chem. 13* (1948) 144.
9. Cotton, F. A. and Wilkinson, G. *Advanced Inorganic Chemistry,* 4th Edn., John Wiley and Sons, New York 1980.
10. Jeffery, G. H., Bassett, G., Mendham, J. and Denney, R. C. *Vogel's Textbook of Quantitative Chemical Analysis,* 5th Edn., Longman, Avon 1989, pp. 186 and 311.
11. Ginstrup, O. *Chem. Instrum. 4* (1973) 141.
12. Sjöberg, S., Hägglund, Y., Nordin, A. and Ingri, N. *Marine Chem. 13* (1983) 35.
13. Ingri, N. and Sillen, L. G. *Arkiv. Chem. 23* (1964) 97.
14. Arnek, R., Sillen, L. G. and Wahlberg, O. *Arkiv. Chem. 31* (1969) 353.
15. Brauner, P., Sillen, L. G. and Whiteker, R. *Arkiv. Chem. 31* (1969) 365.
16. Sigmaplot Scientific Graphing System Version 4.0, Jandel Corporation, 1986–1989.
17. Hietapelto, V., Laitinen, R. S., Pursiainen, J. and Rahkamaa, E. *Acta Chem. Scand.* (1998). *In press.*
18. Baes, C. F. and Mesmer, R. E. *The Hydrolysis of Cations,* 1st Edn., John Wiley and Sons, New York 1976, pp. 241, 246 and 293.
19. Eriksson, G. *Anal. Chim. Acta 112* (1979) 375.

20. Rossotti, H. S. *Talanta 21* (1974) 809.
21. Moore, P. and Buck, D. M. W. *J. Chem. Soc., Dalton Trans.* (1973) 1602.
22. Chattopadhyay, P. K. and Coetzee, J. F. *Inorg. Chem. 12* (1973) 113.
23. Irving, H. and Williams, R. J. P. *Nature (London) 162* (1948) 746.
24. Irving, H. and Williams, R. J. P. *J. Chem. Soc.* (1953) 3192.
25. Bersuker, B. *Coord. Chem. Rev. 14* (1975) 357.
26. James, B. and Williams, R. *J. Chem. Soc.* (1961) 2007.
27. Schwarz, H., Creutz, C. and Sutin, N. *Inorg. Chem. 24* (1985) 433.

28. Yasuda, M., Sone, K. and Yamasaki, K. *J. Phys. Chem. 60* (1956) 1667.
29. Perkampus, H. H. and Köhler, H. in *DMS UV ATLAS of Organic Compounds*, Vol. 2, Verlag Chemie, Weinheim 1966, G10/1–3.
30. Cohen, M. D. and Fischer, E. *J. Chem. Soc.* (1962) 3044.
31. Nowicka-Jankowska, T. *J. Inorg. Nucl. Chem. 33* (1971) 2043.
32. Stynes, D. V. *Inorg. Chem. 14* (1975) 453.